Electronic Supplementary Information

Unravelling the Polydopamine Mystery: Is the End in Sight?

Qinghua Lyu+, Nathanael Hsueh+, and Christina L. L. Chai*.

Department of Pharmacy, National University of Singapore, 18 Science Drive 4, Singapore 117543.

*Corresponding author: E-mail: phacllc@nus.edu.sg; Tel: +65 6601 1061; Fax: +65 6779 1554.

+These authors contributed equally to this work.

1. MALDI-MS of PDA-coatings Derived from Unlabeled DA

The MALDI-MS spectrum of PDA derived from unlabeled DA revealed an intense peak at *m/z* 402 in the presence of Tris[1] or phosphate buffer (**Figure S1**).[2-3]

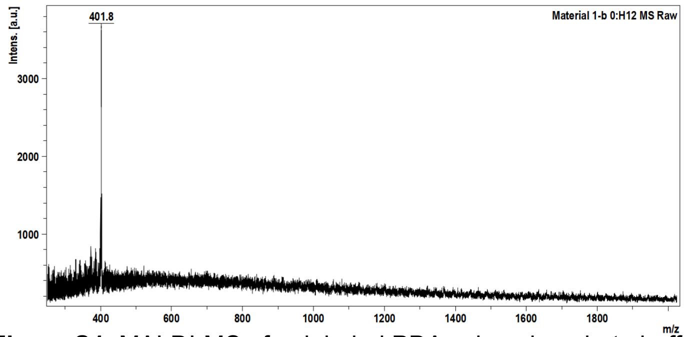

Figure S1. MALDI-MS of unlabeled PDA using phosphate buffer.

2. ESI-MS of Aqueous DA Undergoing Oxidative Polymerization

ESI-MS was utilized to characterize the species present in solution during the oxidative polymerization of unlabeled and deuterium-labeled DA (10 mM, Tris buffer, pH 8.5) at different time points ranging from 5 min to 2 hrs (**Figure S2**).

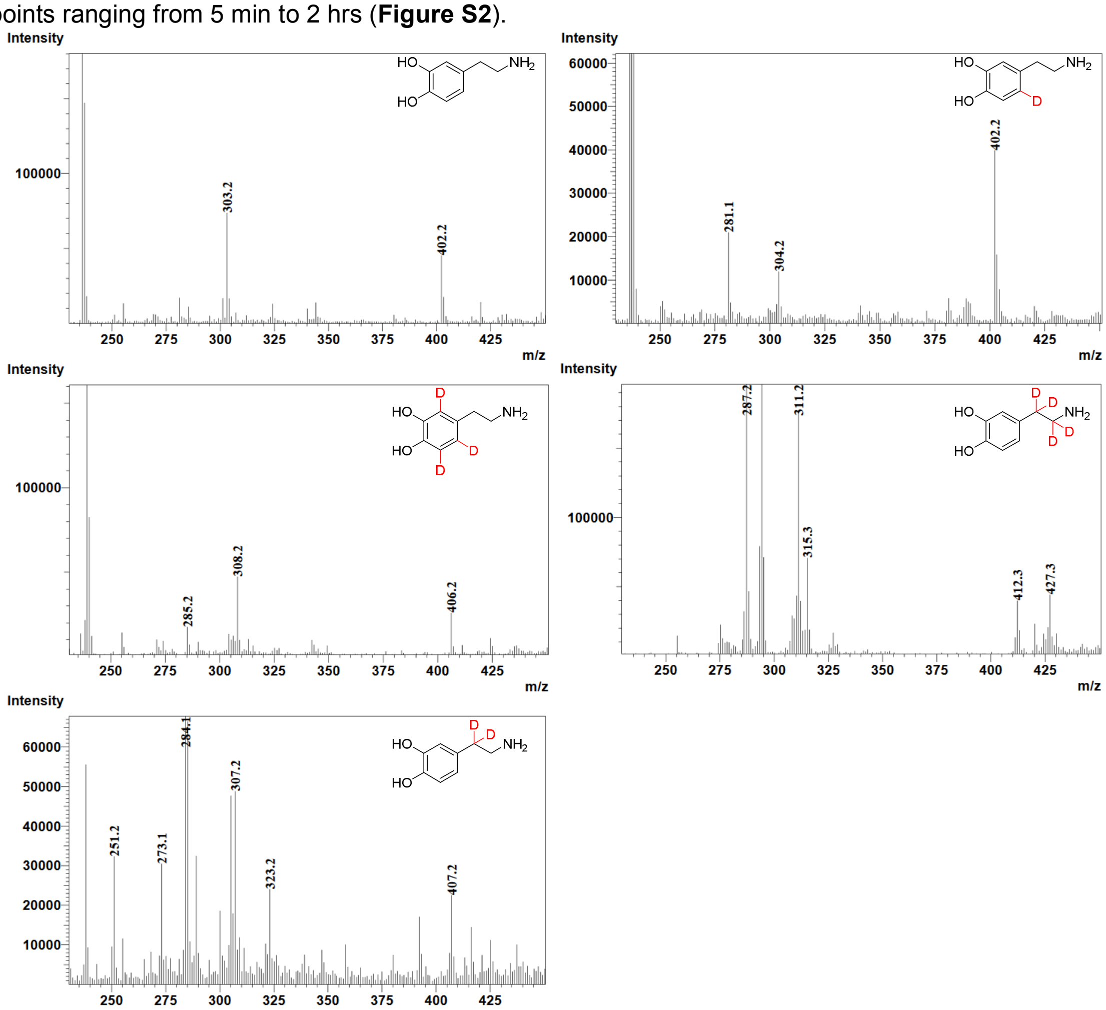

Figure S2. ESI-MS spectra of the oxidative polymerization of DA in solution (< 2hrs).

Times longer than 2 hrs were not suitable, as precipitate formation clogged the ESI-MS, while filtering the solution appeared to remove the oligomers related to the trimer (*m/z* 402 in unlabeled DA). When unlabeled DA was used, *m/z* 402 was detected within 5 min. Another peak at *m/z* 420 was always observed, which was assigned to be the H_2O adduct. The mobile phase used for the mass spectroscopic experiment affected the ion intensity. The use of H_2O/MeCN as eluent gave more intense peaks at *m/z* 402 and 420 (unlabeled DA) during ESI-MS, compared to the use of H_2O/MeOH as eluent. This could be related to the different solubility of PDA oligomers in different organic solvents.

The ESI-MS of unlabeled DA, fully aryl-deuterated DA (DA-2,5,6$_{ring}$-d_3), and fully alkyl-deuterated (DA-α,α',β,β'-d_4) were also monitored over time under Tris, pH 8.5 (**Figure S3**), and there was no observable H/D exchange at the aryl or alkyl positions, consistent with previous literature.[4]

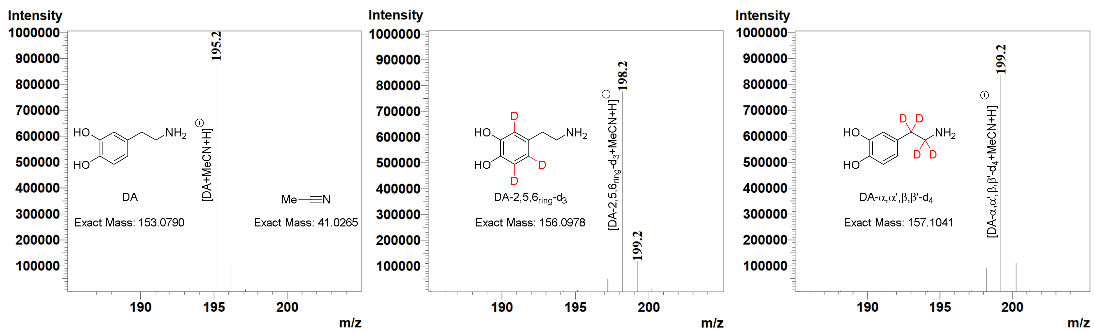

Figure S3. ESI-MS spectra showing absence of H/D exchange at alkyl and aryl positions of DA (Tris, pH 8.5, 1 hr 50 min).

3. ^{1}H NMR and ESI-MS of DA/5,6-dihydroxyindoline or DA/DHI mixtures

A mixture of DA and 5,6-dihydroxyindoline·HBr (**3**·HBr) (10 mM: 5 mM) was dissolved in D_2O, and deuterated Tris-d_{11} (10 mM final concentration) added (**Figure S4A**). This mixture was then analyzed *via* ^{1}H NMR spectroscopy at various time-points. 5,6-dihydroxyindoline·HBr (5 mM) dissolved in D_2O, in the presence and absence of deuterated Tris-d_{11} (10 mM) was used as a comparison (**Figure S4B**). In the presence of DA, the DAC formed was stable and did not decay much (<15%) over a period of 1.5 hrs (**Figure S4A**). **Figure S4A** also shows that the alkyl and aryl protons of DAC have shifted and broadened in the presence of DA (compare with **Figure S4B (ii)**, where there is no DA), strongly suggesting the formation of the DA/DAC complex **5**. Without Tris, 5,6-dihydroxyindoline does not convert into DAC (**Figure S4B (i)**). Upon addition of Tris, DAC was formed rapidly (**Figure S4B (ii)**), and after 1.5 hrs, 37% had decayed into DHI (**Figure S4B (iv)**). This suggests that the DA/DAC complex formed is relatively stable.

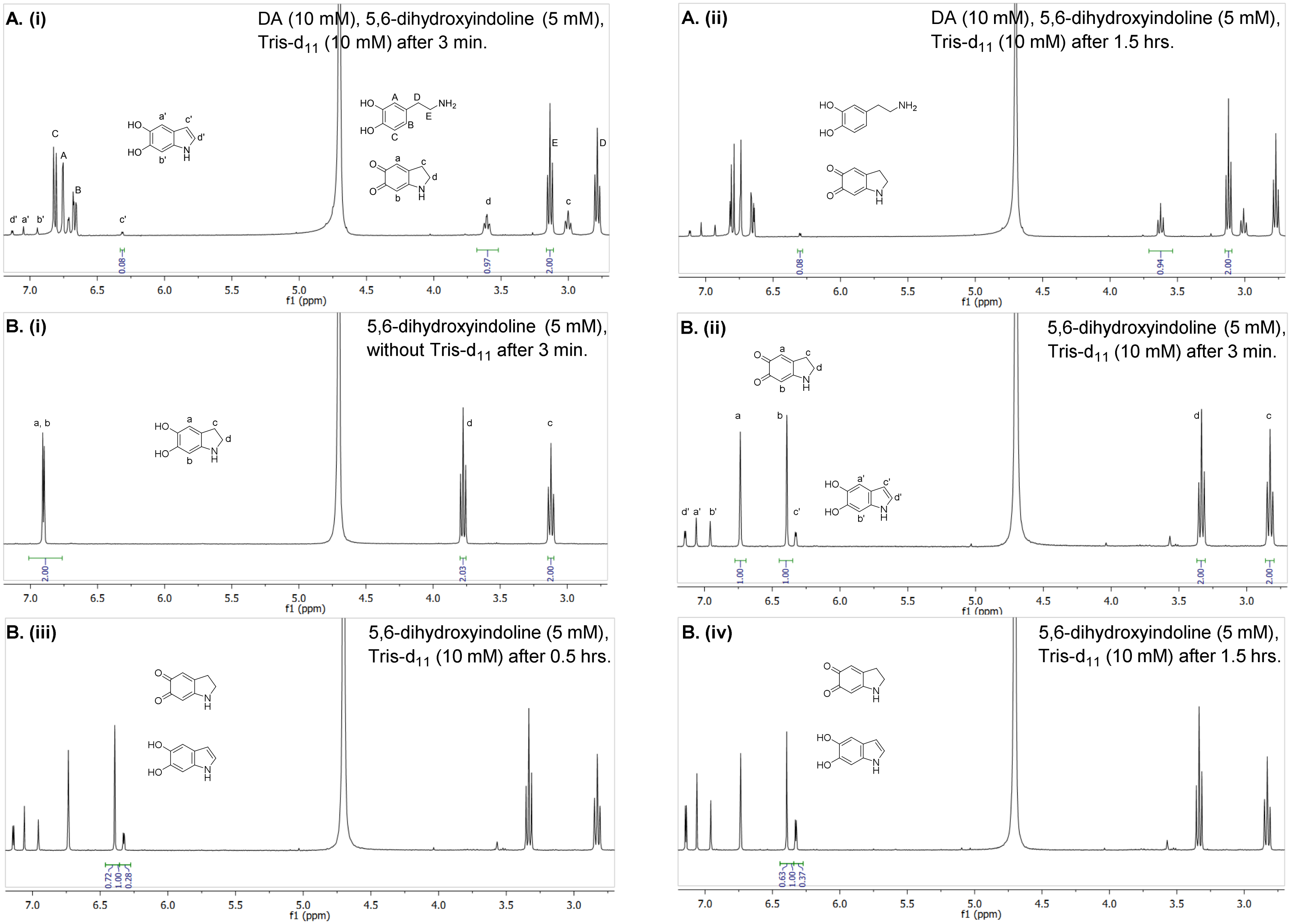

Figure S4. [1]H NMR of: (**A**) DA/5,6-dihydroxyindoline with Tris; (**B**) 5,6-dihydroxyindoline with and without Tris.

A mixture of DA and 5,6-dihydroxyindoline·HBr (**3**·HBr) (10 mM:1 mM, or 10 mM:10 mM) in Tris (10 mM, pH 8.5) was analyzed under ESI-MS after 5 min (no shaking, standard atmospheric conditions), giving a peak at *m/z* 303 (**Figure S5**). When the mixture was shaken continously under standard atmospheric conditions for 10 min, the peak at *m/z* 285 grew in intensity.

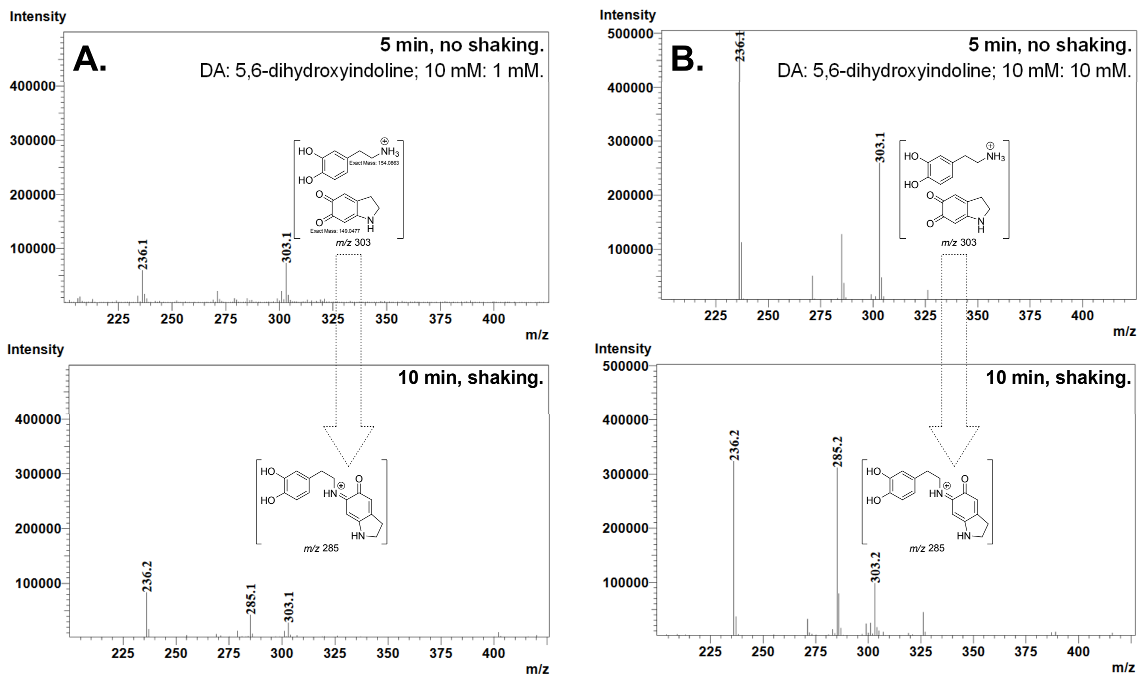

Figure S5. ESI-MS spectra of DA/5,6-dihydroxyindoline; (**A**) 10 mM: 1 mM, (**B**) 10 mM: 10mM.

A mixture of DA/DHI (10 mM:1 mM, or 10 mM:10 mM) in Tris (10 mM, pH 8.5) was analyzed *via* ESI-MS (**Figure S6**) after 5 min (no shaking, standard atmospheric conditions); no significant peak at *m/z* 303 was seen.

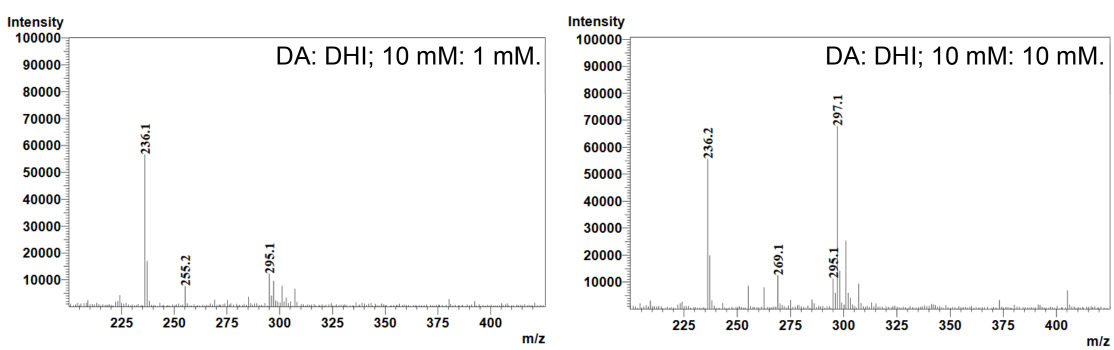

Figure S6. ESI-MS spectra of DA/DHI.

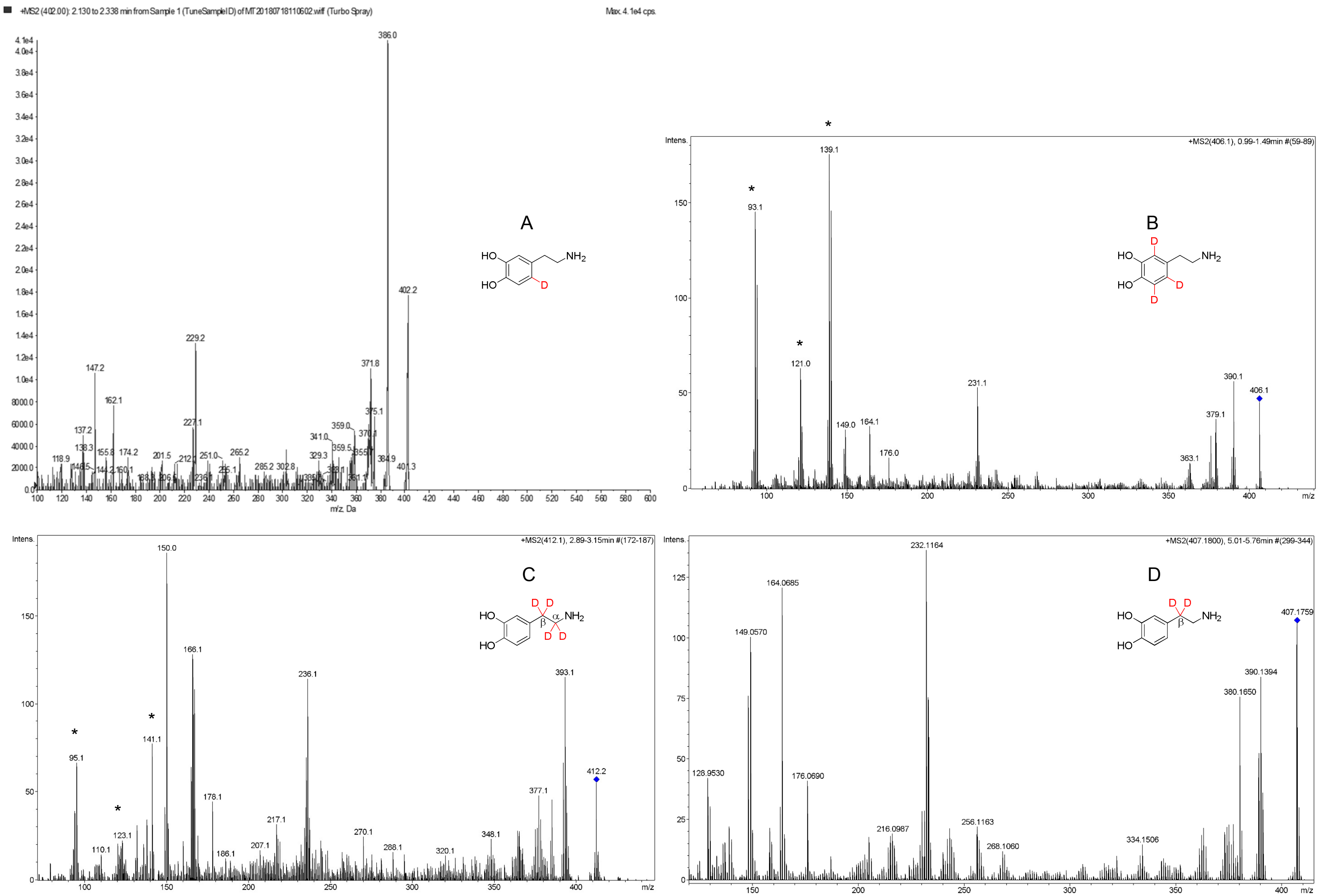

Figure S7. ESI-MS^2 of parent ions at: (**A**) *m/z* 402 (DA-6$_{ring}$-d$_1$); (**B**) *m/z* 406 (DA-2,5,6$_{ring}$-d$_3$); (**C**) *m/z* 412 (DA-α,α',β,β'-d$_4$); (**D**) *m/z* 407 (DA-β,β'-d$_2$).

4. ESI-MS^2 of Parent Ions Derived from Deuterated DA

Tandem MS^2 experiments on *m/z* 402, 406, 412, and 407 (using DA-6$_{ring}$-d$_1$, DA-2,5,6$_{ring}$-d$_3$, DA-α,α',β,β'-d$_4$, and DA-β,β'-d$_2$ respectively) revealed the same fragmentation pattern (**Figure S7**). Due to the lower intensities of the parent ions, perhaps because of C–D/C–H kinetic isotope effect on oxidation and polymerization kinetics, the signal to noise ratio was lower compared to the tandem MS^2 experiment on unlabeled *m/z* 402. Fragment ions from deuterium-labeled DA (marked asterisk) were also observed with *m/z* 406 (DA-2,5,6$_{ring}$-d$_3$) and *m/z* 412 (DA-α,α',β,β'-d$_4$) due to the lower signal to noise ratio.

5. Additional Discussion on F_1 – F_5

The tandem MS^2 experiments indicated that the trimer responsible for *m/z* 402 contained 4 aryl- and 10 alkyl- protons that had been preserved from the starting DA monomer, according to the distribution $2H_{aryl}$+ $2H_{aryl}$ +0, and $4H_{alkyl}$ +$3H_{alkyl}$ +$3H_{alkyl}$.

F_1 at *m/z* 386.1139 ($C_{22}H_{16}N_3O_4$) is derived from the parent ion (*m/z* 402.1447, $C_{23}H_{20}N_3O_4$) by a loss of CH_4 (16 Da). A loss of 17 Da and 19 Da respectively from *m/z* 407 (using DA-β,β'-d$_2$) and *m/z* 412 (using DA-α,α',β,β'-d$_4$) indicated the lost CH_4 contains 2 $α_{alkyl}$-H and 1 $β_{alkyl}$-H. This fragmentation pattern may suggest that the parent ion contains one methyl group, generated *via* the breakdown of of the side chain during the polymerization of DA. Furthermore, one $H_β$ migrated to this methyl unit during this process (**Figure S8**). However, we were unable to find any evidence or prior literature to support such a pathway during the oxidative polymerization of DA. A more plausible explanation is that a loss of [C[$H_α$]$_2$+$H_β$+H] occurs only under ESI-MS^2 conditions.

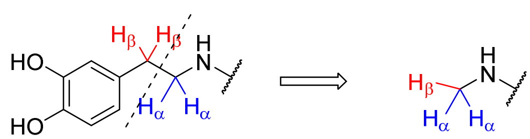

Figure S8. Hypothetical side-chain breakdown to form a methyl unit containing 2 $α_{alkyl}$-H and 1 $β_{alkyl}$-H.

F_2 at *m/z* 375.1366 ($C_{22}H_{19}N_2O_4$) is derived from the parent ion (*m/z* 402.1447) by a loss of HCN (27 Da), a typical fragmentation pattern of aniline or aromatic heterocyclic compounds, e.g. pyridine and indole.[5-9] **Figure S9** shows the structural units that could account for this loss of 27 Da. Motifs **A** and **B** (**Figure S9**) are more likely to be present in the parent ion, as opposed to **C** and **D**, because the same loss of 27 Da occurred from all parent ions regardless of deuteration pattern, indicating that the lost proton in HCN was not derived from the alkyl-H or aryl-H of DA.

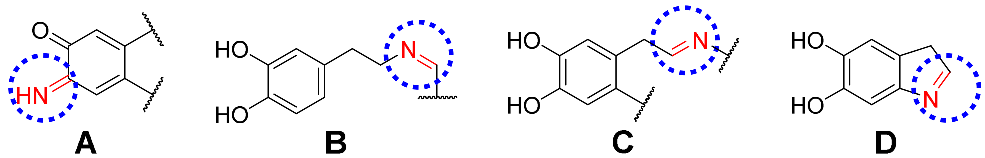

Figure S9. Possible functionalities accounting for a loss of HCN in *m/z* 402.

$\mathbf{F_4}$ is found at *m/z* 162.0552 ($C_9H_8NO_2$) with unlabeled DA. Use of DA-2,5,6$_{ring}$-d_3 and DA-α,α',β,β'-d_4 give *m/z* 164 and *m/z* 166 respectively, indicating the presence of 2 aryl-H and 4 alkyl-H. Possible structures accounting for $\mathbf{F_4}$ are 6-*O*-methylene dopaminochrome, *N*-methylene dopaminochrome or tetrahydroisoquinoline (TIQ) (**Figure S10A**). However, the parent ion is unlikely to contain the TIQ motif, because dopamine-derived TIQ derivatives such as salsolinol reported in literature do not show such fragmentation patterns under ESI-MS/MS conditions.[10-11]

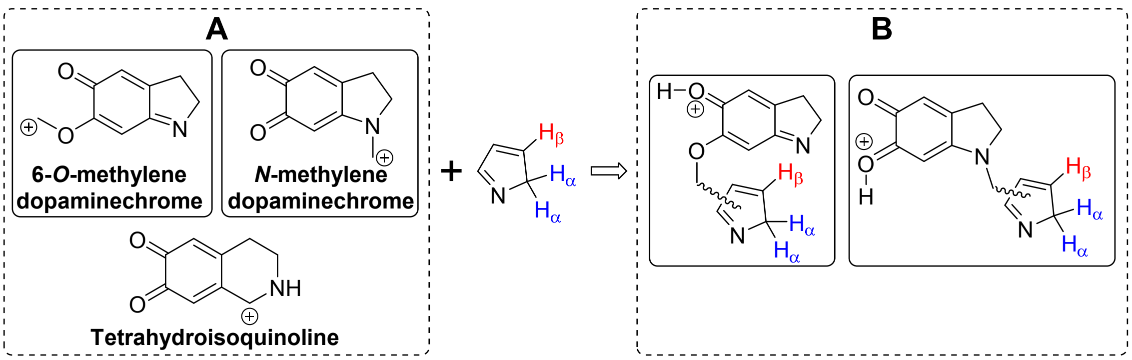

Figure S10. Possible structures of $\mathbf{F_4}$ (**A**) and $\mathbf{F_3}$ (**B**).

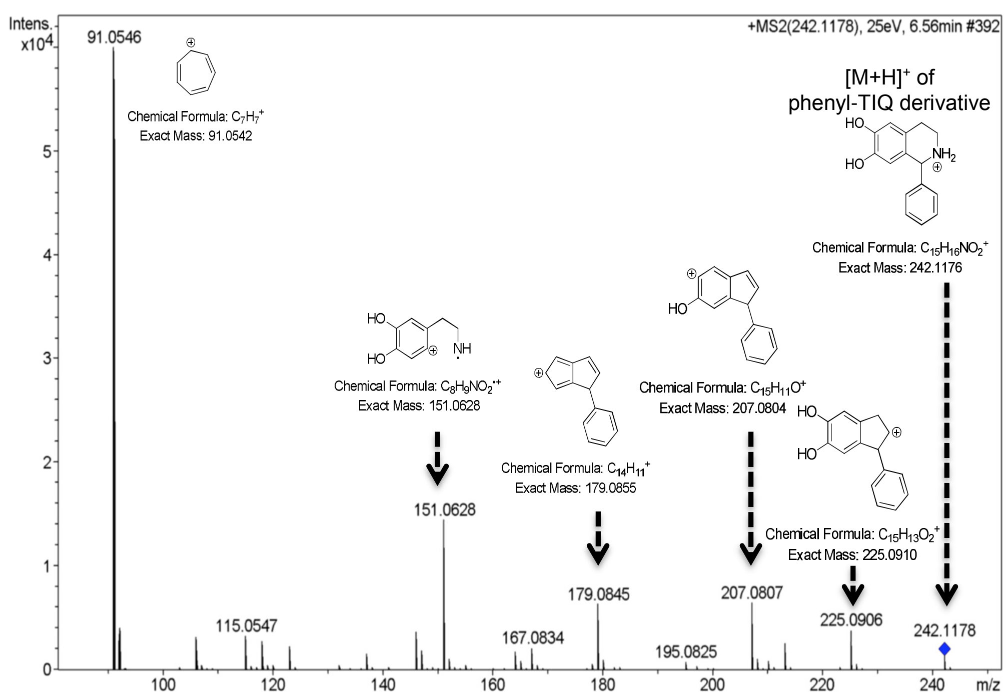

Figure S11. HR-ESI-MS^2 of a phenyl-TIQ derivative.

To further verify this, a phenyl-substituted, dopamine-derived TIQ derivative was synthesized using DA,[12] and ESI-MS^2 analysis revealed a loss of NH_3 rather than a loss of the phenyl group (**Figure S11**).

Similarly, $\mathbf{F_3}$ at *m/z* 229.0992 ($C_{13}H_{13}N_2O_2$) is deduced to contain 2 aryl-H and 7 alkyl-H, and is a combination of $\mathbf{F_4}$ (*m/z* 162.0552, $C_9H_8NO_2$) and C_4H_5N unit (67 Da, 2*H*-pyrrole) (**Figure S10B**) This proposal is supported by the mass difference between unlabeled/deuterium-labeled $\mathbf{F_3}$ and $\mathbf{F_4}$. $\mathbf{F_3}$ and $\mathbf{F_4}$ have a mass difference of 67 Da using DA-2,5,6$_{ring}$-d$_3$ ($\mathbf{F_3}$ at *m/z* 231, $\mathbf{F_4}$ at *m/z* 164), the same difference as that between unlabeled $\mathbf{F_3}$ (*m/z* 229) and $\mathbf{F_4}$ (*m/z* 162). This indicates that the C_4H_5N unit does not contain any aryl-H. Use of DA-α,α',β,β'-d$_4$ gave a mass difference of 70 Da between $\mathbf{F_3}$ and $\mathbf{F_4}$ (*m/z* 236 and *m/z* 166 respectively), indicating that C_4H_5N has 3 alkyl-H preserved. Further experiments with DA-β,β'-d$_2$ ($\mathbf{F_3}$ and $\mathbf{F_4}$ at *m/z* 232 and *m/z* 164 respectively; difference of 68 Da) showed that the 3 alkyl-H in C_4H_5N is comprised of one H_β and two H_α. Possible structures of $\mathbf{F_3}$ are shown in **Figure S10B**.

$\mathbf{F_5}$ at *m/z* 147.0491 ($C_9H_7O_2$) was shown *via* deuterium labeling to contain 2 aryl-H and 3 alkyl-H (one H_α and two H_β). Possible structures of $\mathbf{F_5}$ are showed in **Figure S12A**. Loss of H_α may occur during oxidative polymerization, *via* tautomerization of the quinone-imine at the α position of the side chain to give aromatic Schiff-base as shown in **Figure S12B**. $\mathbf{F_5}$ ($C_9H_7O_2$; 2 aryl-H + 3 alkyl-H) and $\mathbf{F_3}$ ($C_{13}H_{13}N_2O_2$; 2 aryl-H + 7 alkyl-H) together account for $\mathbf{F_2}$ ($C_{22}H_{19}N_2O_4$; 4 aryl-H + 10 alkyl-H), as supported by all deuterium-labeled MS data.

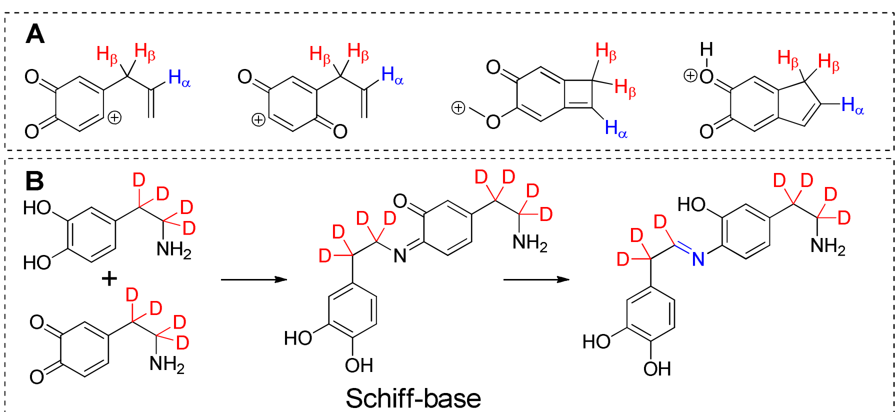

Figure S12. (**A**) Possible structures of $\mathbf{F_5}$; (**B**) possible pathway involving one D_α loss in the polymerization of DA-α,α',β,β'-d$_4$.

6. Synthetic Methods

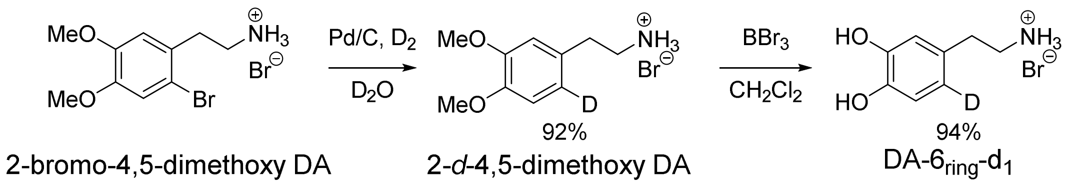

Scheme S1. Synthesis of DA-6$_{ring}$-d$_1$.

Synthesis of DA-6$_{ring}$-d$_1$. The compound was synthesized following **Scheme S1**. Palladium on carbon (10 wt. %, 33 mg, 0.031 mmol) was added to D_2O (5.53 g, 276 mmol) in a 100 mL round-bottom flask. The flask was evacuated and filled with H_2(g), then stirred at r.t. for 24 hrs to generate D_2 (g).[13] 2-bromo-4,5-dimethoxy DA[14] (80 mg, 0.235 mmol) dissolved in D_2O (1 mL) was then added and the reaction mixture stirred at r.t. for a further 20 hrs. The mixture was then filtered, residue rinsed with cold MeOH, and the solution concentrated under vacuum. 2-*d*-4,5-dimethoxy DA (58 mg, 92% yield) was obtained as a light yellow solid. ^{1}H-NMR (400 MHz, D_2O) δ (ppm): 7.02 (t, $^2J_{HD}$=4.7 Hz, 1H), 6.98 (s, 1H), 3.86 (s, 3H), 3.84 (s, 3H), 3.26 (m, 2H), 2.95 (t, *J*=73.Hz, 2H). ESI-MS: *m/z* calcd for $C_{10}H_{14}DNO_2$ [M+1]$^+$ 183.12, found 183.11.

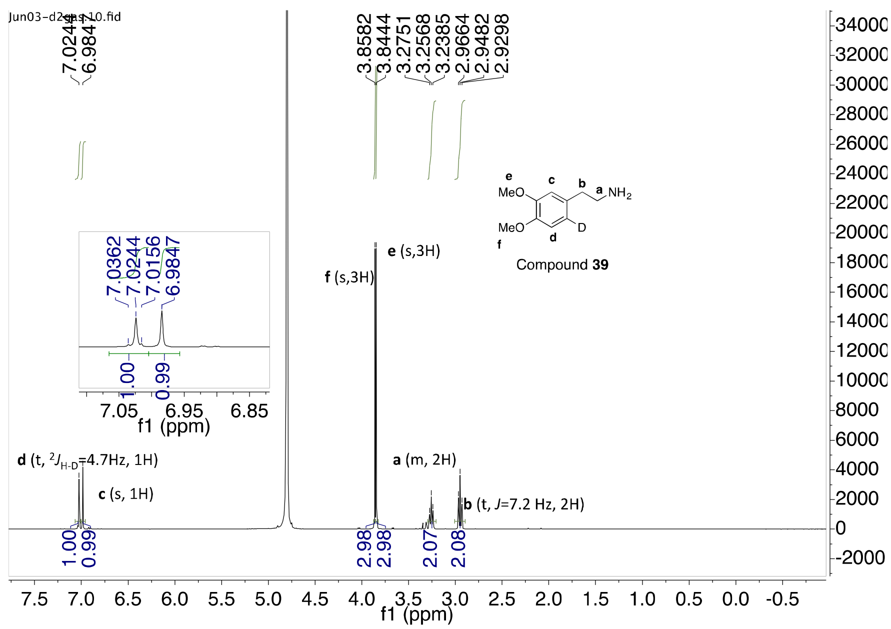

Figure S13. ^{1}H-NMR spectrum of 2-*d*-4,5-dimethoxy DA.

To a cooled (0 °C) mixture of 2-*d*-4,5-dimethoxy DA (52 mg, 0.20 mmol) in anhydrous CH_2Cl_2 (5 mL) was added BBr_3 (0.12 mL, 1.2 mmol) dissolved in CH_2Cl_2 (1 mL) dropwise. The mixture was allowed to warm to r.t. and stirred for 4 hrs. The precipitate was collected under centrifugation and washed with heptane (5 mL) and CH_2Cl_2 (5 mL). The precipitate was then suspended in CH_2Cl_2 (5 mL), and 7 M NH_3 in MeOH added dropwise until pH≈5. The NH_4Br produced was then filtered off, and the solution was concentrated under vacuum to give DA-6_{ring}-d_1 (45 mg, 94% yield) as a white solid. ^{1}H-NMR (400 MHz, CD_3OD) δ (ppm): 6.74 (t, $^2J_{HD}$= 3.4 Hz, 1H), 6.69 (s, 1H), 3.10 (m, 2H), 2.80 (t, J= 7.8Hz, 2H); ESI-MS: m/z calcd for $C_8H_{10}D_1NO_2$ $[M+1]^+$ 154.09, found 154.10.

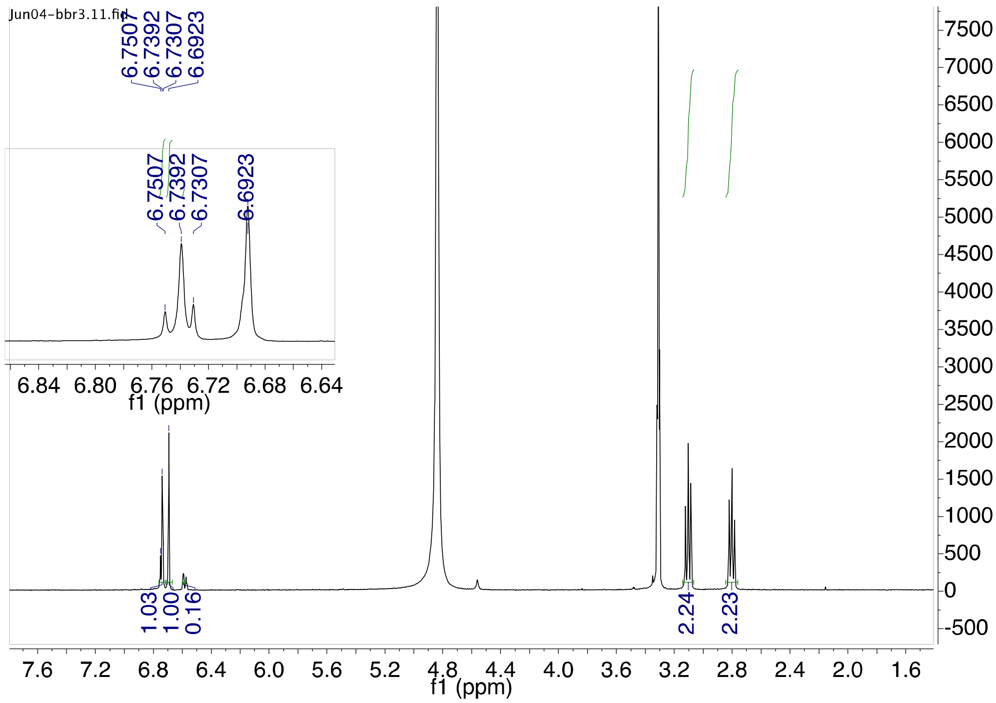

Figure S14. ^{1}H-NMR spectrum of DA-6_{ring}-d_1.

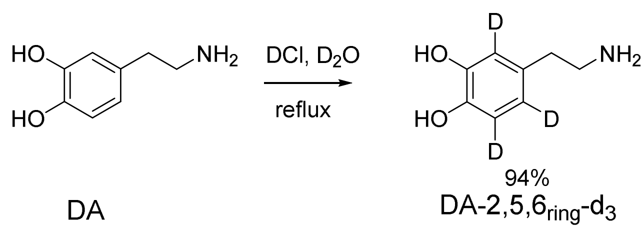

Scheme S2. Synthesis of DA-2,5,6_{ring}-d_3.

Synthesis of DA-2,5,6_{ring}-d_3. The compound was synthesized following **Scheme S2**. Dopamine·HCl (100 mg, 0.527 mmol) dissolved in 6 M DCl/D_2O (2 mL) was heated at reflux under a nitrogen atmosphere for 6 hrs. The solution was then concentrated under vacuum to give a white residue, which was subsequently redissolved in MeOH to exchange labile hydroxyl and amine deuteriums. Removal of solvents under vacuum gave DA-2,5,6_{ring}-d_3 (105 mg, 94% yield) as a white solid.[4] ^{1}H-NMR (CD_3OD): δ (ppm) 3.10 (m, 2H), 2.80 (m, 2H); ESI-MS: m/z calcd for $C_8H_8D_3NO_2$ $[M+1]^+$ 157.09, found 157.10.

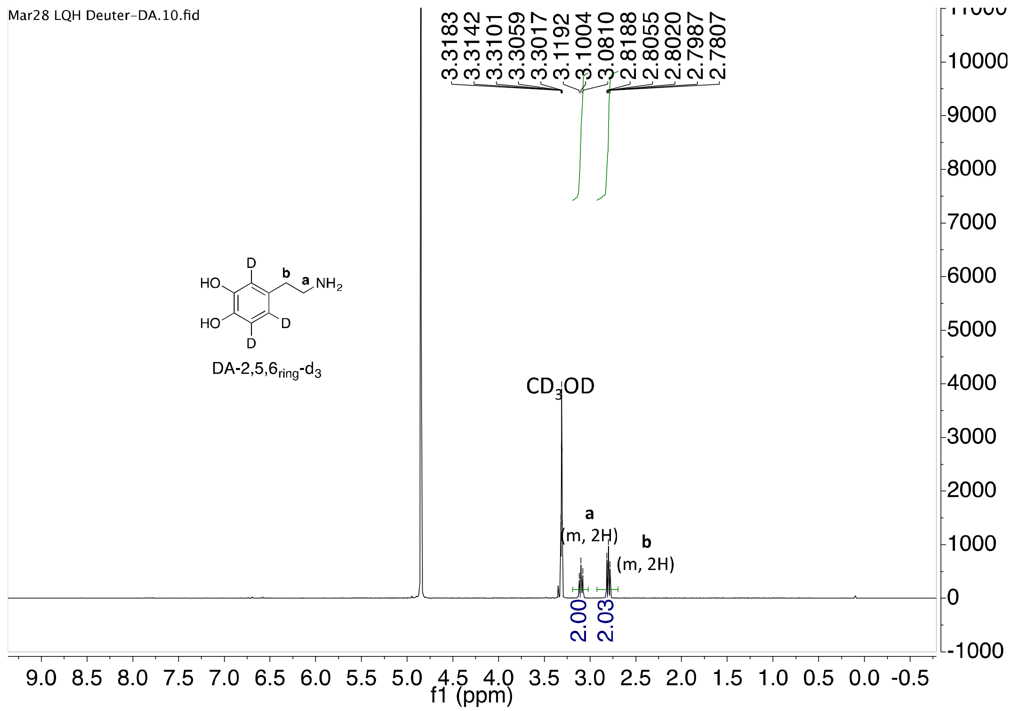

Figure S15. ^{1}H-NMR spectrum of DA-2,5,6$_{ring}$-d$_3$.

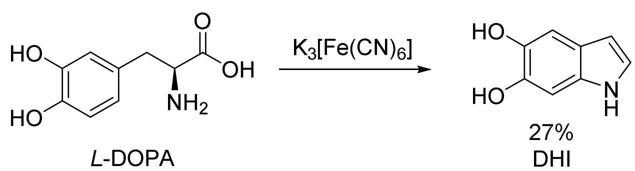

Scheme S3. Synthesis of DHI.

Synthesis of 5,6-Dihydroxyindole (DHI). DHI was prepared under nitrogen atmosphere using the reported method (**Scheme S3**).[15] A mixture of $K_3[Fe(CN)_6]$ (6.6 g, 20 mmol) and $NaHCO_3$ (2.5 g, 30 mmol) in H_2O (60 mL) was added dropwise over 5 min to a stirred solution of *L*-DOPA (0.99 g, 5 mmol) in H_2O (500 mL). The resulting solution was stirred at room temperature under nitrogen atmosphere for 3 hrs, then $Na_2S_2O_4$ (600 mg) added. The solution was then adjusted to pH 4 with aq. 3 M HCl and extracted with EtOAc (3 × 250 mL). The combined organic extracts were washed with saturated aq. NaCl (3 × 100 mL), dried over Na_2SO_4, then concentrated under vacuum to approximately 5 mL. Addition of hexane (50 mL) to the residue yielded a pale brown solid, which was subsequently recrystallized from EtOAc/hexane. DHI (287 mg, 27% yield) was obtained as an off-white solid. ^{1}H-NMR (CD_3OD): δ (ppm) 6.21 (d, J= 3.08 Hz, 1H), 6.88 (s, 1H), 6.96 (s, 1H), 7.04 (d, J=3.08 Hz, 1H).

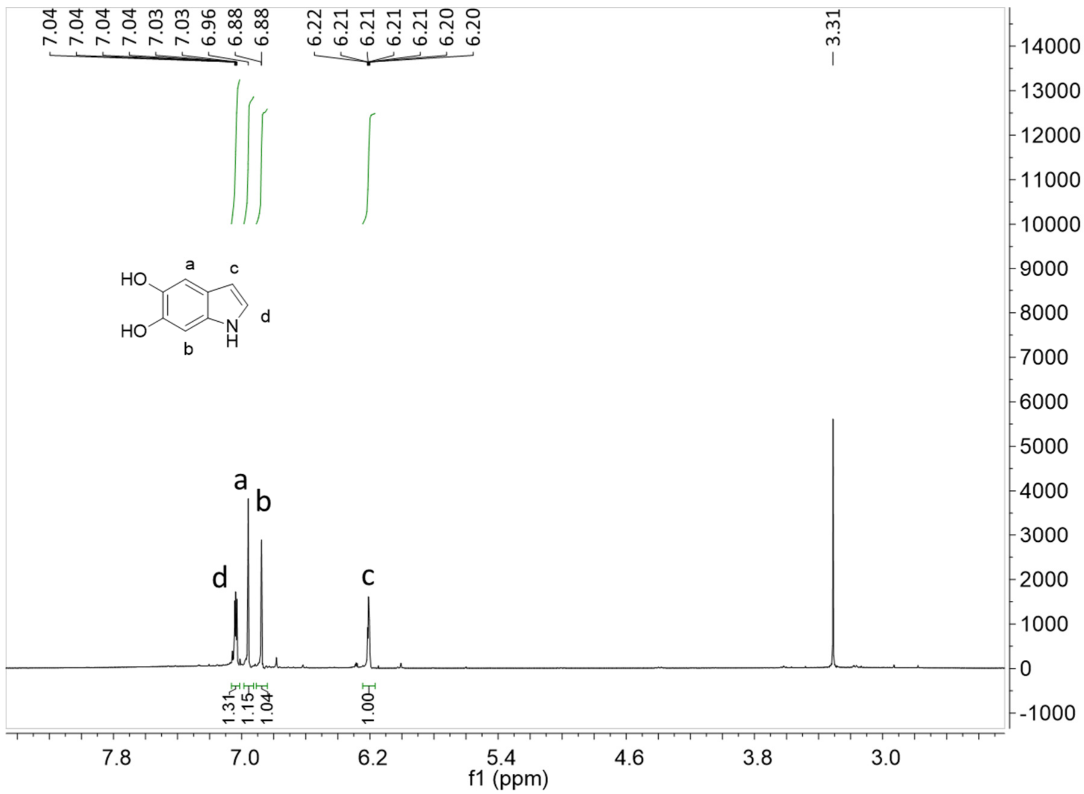

Figure S16. ^{1}H-NMR spectrum of DHI.

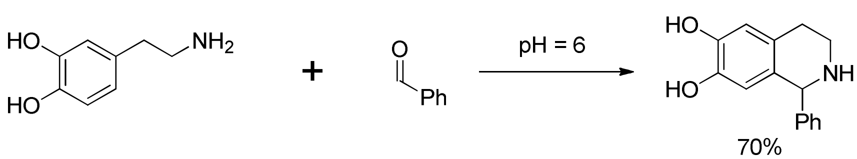

Scheme S4. Synthesis of a phenyl-TIQ derivative.

Synthesis of Phenyl-TIQ Derivative. Phenyl-TIQ derivative was synthesized according to literature procedures (**Scheme S4**).[12] Dopamine (0.100 g, 0.527 mmol) was dissolved in a mixture of potassium phosphate buffer (0.1M, pH 6, 5 mL) and MeCN (5 mL). Benzaldehyde (130 µL, 1.3 mmol) was added, and the solution stirred at 50°C for 24 hrs. The brown solution was then concentrated under vacuum, and the residue was subjected to reverse phase column chromatography (1% MeOH in H_2O) to give the phenyl-TIQ derivative as a white solid (0.089 g, 70% yield). ^{1}H-NMR (400 MHz; D_2O) δ (ppm): 7.44-7.41 (m, 3H), 7.30-7.28 (m, 2H), 6.78(s, 1H), 6,32 (s, 1H), 5.6 (s, 1H), 3.45-3.32 (m, 2H), 3.10-2.96 (m, 2H). ESI-MS: *m/z* calcd for $C_{15}H_{16}NO_2$ $[M+1]^+$ 242.12, found 242.20.

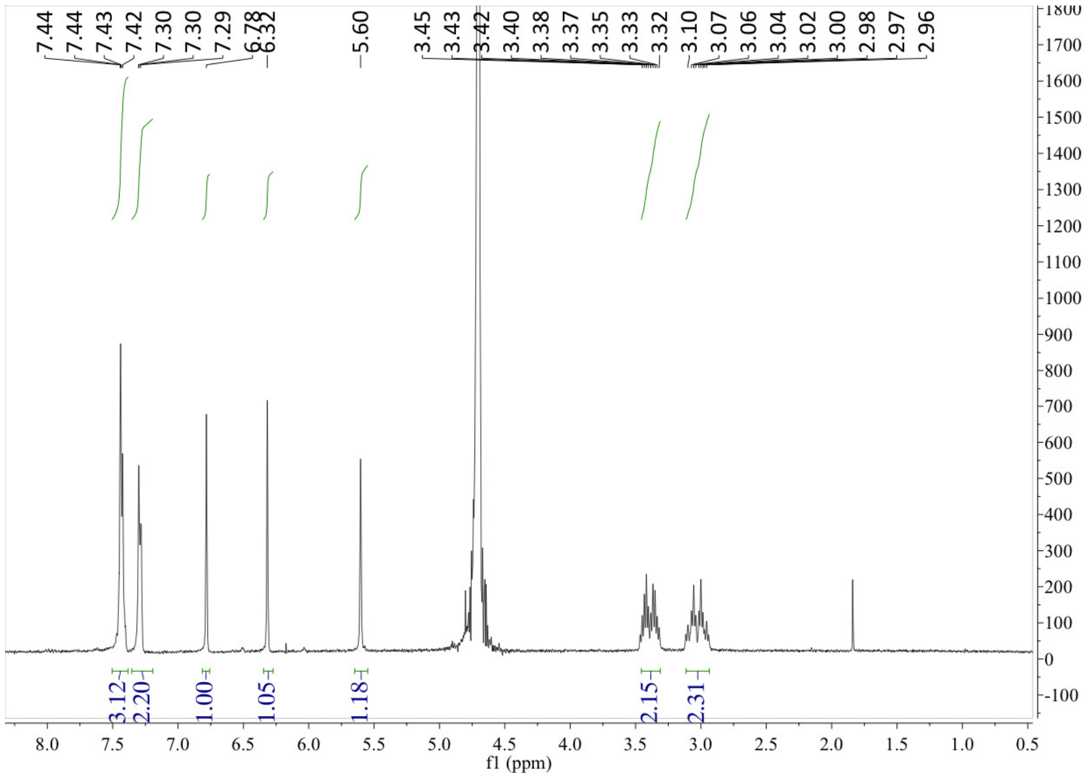

Figure S17. ^{1}H-NMR spectrum of phenyl-TIQ derivative.

7. References

1. Lyu, Q.; Hsueh, N.; Chai, C. L. L. Direct Evidence for the Critical Role of 5,6-Dihydroxyindole in Polydopamine Deposition and Aggregation. *Langmuir* **2019,** *35*, 5191–5201, DOI: 10.1021/acs.langmuir.9b00392.

2. Ding, Y.; Weng, L.-T.; Yang, M.; Yang, Z.; Lu, X.; Huang, N.; Leng, Y. Insights into the Aggregation/Deposition and Structure of a Polydopamine Film. *Langmuir* **2014,** *30*, 12258–12269, DOI: 10.1021/la5026608.

3. Alfieri, M. L.; Micillo, R.; Panzella, L.; Crescenzi, O.; Oscurato, S. L.; Maddalena, P.; Napolitano, A.; Ball, V.; d'Ischia, M. Structural Basis of Polydopamine Film Formation: Probing 5,6-Dihydroxyindole-Based Eumelanin Type Units and the Porphyrin Issue. *ACS Appl. Mater. Interfaces* **2018,** *10*, 7670–7680, DOI: 10.1021/acsami.7b09662.

4. Pająk, M.; Kańska, M. Synthesis of isotopomers of dopamine labeled with deuterium or tritium. *J. Label. Compd. Radiopharm.* **2006,** *49*, 1061–1067, DOI: 10.1002/jlcr.1123.

5. Eberlin, M. N.; Augusti, D. V.; Augusti, R. Mass Spectrometry and Gas‐Phase Chemistry of Anilines. In: *PATAI'S Chemistry of Functional Groups*. Rappoport, Z. Ed. (John Wiley & Sons, Ltd., 2009), DOI: 10.1002/9780470682531.pat0387.

6. Corval, M. An electron impact study of HCN elimination from indole by use of 13C labelling. *Org. Mass Spectrom.* **1981,** *16*, 444–447, DOI: 10.1002/oms.1210161005.

7. Draper, P. M.; MacLean, D. B. Mass spectra of alkylquinolines. *Can. J. Chem.* **1968,** *46*, 1487–1497, DOI: 10.1139/v68-245.

8. Baldwin, M. A.; Gilmore, J.; Mruzek, M. N. Unexpected structural integrity of gas phase isoquinoline cations that eliminate HCN. *Org. Mass Spectrom.* **1983,** *18*, 127–129, DOI: 10.1002/oms.1210180308.

9. Fischer, G. The Chemistry of Pyrido[1,2-a]azepines and Their Hydro Derivatives. In: *Advances in Heterocyclic Chemistry*. Katritzky, A. Ed. (Academic Press, 2011), Vol. 103, pp 61–174, DOI: 10.1016/B978-0-12-386011-8.00002-2.

10. Cai, M.; Liu, Y. M. Quantification of salsolinol enantiomers by stable isotope dilution liquid chromatography with tandem mass spectrometric detection. *Rapid Commun. Mass Spectrom.* **2008,** *22*, 4171–4177, DOI: 10.1002/rcm.3847.

11. Song, Y.; Xu, J.; Hamme, A.; Liu, Y.-M. Capillary liquid chromatography–tandem mass spectrometry of tetrahydroisoquinoline derived neurotoxins: A study on the blood–brain barrier of rat brain. *J. Chromatogr. A* **2006,** *1103*, 229–234, DOI: 10.1016/j.chroma.2005.11.014.

12. Pesnot, T.; Gershater, M. C.; Ward, J. M.; Hailes, H. C. Phosphate mediated biomimetic synthesis of tetrahydroisoquinoline alkaloids. *Chem. Commun.* **2011,** *47*, 3242–3244, DOI: 10.1039/C0CC05282E.

13. Kurita, T.; Aoki, F.; Mizumoto, T.; Maejima, T.; Esaki, H.; Maegawa, T.; Monguchi, Y.; Sajiki, H. Facile and Convenient Method of Deuterium Gas Generation Using a Pd/C‐Catalyzed H_2‐D_2 Exchange Reaction and Its Application to Synthesis of Deuterium‐Labeled Compounds. *Chem. Eur. J.* **2008,** *14*, 3371‐3379, DOI: 10.1002/chem.200701245.

14. Rote, J. C.; Malkowski, S. N.; Cochrane, C. S.; Bailey, G. E.; Brown, N. S.; Cafiero, M.; Peterson, L. W. Catechol reactivity: Synthesis of dopamine derivatives substituted at the 6-position. *Synth. Commun.* **2017,** *47*, 435–441, DOI: 10.1080/00397911.2016.1269350.

15. Charkoudian, L. K.; Franz, K. J. Fe(III)-Coordination Properties of Neuromelanin Components: 5,6-Dihydroxyindole and 5,6-Dihydroxyindole-2-carboxylic Acid. *Inorg. Chem.* **2006,** *45*, 3657–3664, DOI: 10.1021/ic060014r.